



e-ISSN:2582-7219



INTERNATIONAL JOURNAL OF MULTIDISCIPLINARY RESEARCH IN SCIENCE, ENGINEERING AND TECHNOLOGY

Volume 6, Issue 3, March 2023



INTERNATIONAL
STANDARD
SERIAL
NUMBER
INDIA

Impact Factor: 7.54



6381 907 438



6381 907 438



ijmrset@gmail.com



www.ijmrset.com



Utility Grid Interfaced Solar WPS Using PMSM Drive

Mrs.R.Punyavathi¹, K S K S Prasad², V.Bhargav³, K.Sai Manikanta⁴, J.Manohar Kumar⁵

Assistant Professor, Department of EEE, KKR & KSR Institute of Technology and Sciences, Guntur,
Andhra Pradesh, India¹

B.Tech Final Year Students, Department of EEE, KKR & KSR Institute of Technology and Sciences, Guntur,
Andhra Pradesh, India²³⁴⁵

ABSTRACT: This work presents a solar water pumping (SWP) system that addresses the intermittency problem of renewable energy sources. The system utilizes an encoder and a grid-fed permanent magnet synchronous motor (PMSM) for continuous water flow even in the absence of sunlight. However, in developing and underdeveloped countries, weak networks are common, and SWP systems deployed at remote locations are susceptible to grid abnormalities. To address this issue, a hybrid multi-resonant generalized integrator-frequency-locked loop (HMRGI-FLL) control structure is proposed in this work. The structure not only rejects DC-offset but also eliminates lower-order harmonics. A boost converter is used to facilitate energy transfer from the grid, and in the event of a network failure, the output water flow is regulated according to solar radiation. Sensorless vector control regulates the PMSM speed. The proposed system's performance is experimentally verified under different conditions, including solar insolation, grid failure, voltage drop, voltage rise, and distorted grid voltage.

KEYWORDS: SWP, PMSM, Sensor-less vector control, Utility grid, Power quality

I.INTRODUCTION

Concerns regarding energy have led researchers to investigate alternative energy solutions to decrease dependence on traditional sources. Recently, various uses have been identified where renewable energy sources (RES) can replace traditional sources. One such area is water pumping, which currently relies heavily on fossil fuels. By using RES for this application, greenhouse gas emissions and carbon footprints can be decreased. Solar photovoltaic (PV) power generation is gaining acceptance due to its modular structure, decreasing installation costs, and zero operating costs. Although a solar PV integrated water pumping system (WPS) provides a viable solution, the intermittent nature of solar energy limits its use to active hours only when solar insolation is available. To effectively use WPS, this drawback must be addressed. Some solutions to this problem include connecting battery energy storage at the DC link, using pump storage and fuel cells as storage mediums. However, these solutions also have their drawbacks, such as increased system complexity, cost, and space requirements. As the grid is an infinite source of energy, integrating the utility grid to solar water pumping (SWP) systems is recommended. This integration enhances system utilization and improves system reliability. A 1- ϕ utility grid interfaced WPS with PFC using a boost DC-DC converter is presented, where the PFC converter maintains the UPF. Additionally, 1- ϕ and 3- ϕ grid interactive WPS with voltage source converters (VSC) at the grid side are also presented. Despite some literature focusing on PFC, none of the existing works address issues related to a weak power grid. The power grid in underdeveloped and developing countries is generally weak, and since most water pumps are located at the radial end of the utility grid, they are susceptible to various power quality (PQ) problems, including voltage sag, voltage swell, grid current distortion, and grid voltage distortion. These PQ issues can impact the performance of WPS and must be resolved for proper operation. PLLs are typically used to synchronize distributed generation systems with the utility grid. However, conventional PLLs can experience harmonic resonance under grid abnormalities due to coupling between the PLL and the grid impedance. In a high impedance network, harmonic current can amplify voltage distortion, leading to system instability. Conventional PLLs are sensitive to frequency variations and harmonic distortions, making it challenging to accurately estimate phase, frequency, and amplitude when the grid voltage is polluted with distortion and DC-offset. Reducing the PLL bandwidth to reject harmonics compromises.

Presently, various techniques in signal processing are being utilized to extract the fundamental component



from distorted grid voltage. This article discusses an enhanced phase-locked loop (EPLL) based on multiple delay signal cancellation (DSC). The EPLL uses a PI controller with gains that require tuning for proper functionality. Additionally, a moving average filter (MAF) with DSC technique is presented to eliminate odd and even order harmonic components. The MAF-based DSC effectively removes smaller magnitude high frequency signals, but filtering larger magnitude high frequency signals requires a larger filter window, resulting in a larger latency in the filtered signal. To address this issue, an adaptive notch filter (ANF) is proposed for filtering distorted signals. Although ANF is effective in eliminating higher order harmonics, it is ineffective in mitigating dominant harmonics. Another synchronization method using vectorial filters is presented where complex coefficients are used for band-pass filtering. A generalized integrator (GI) based quadrature signal generator is widely reported in existing literature for harmonic extraction. Among numerous harmonic extraction techniques, a second-order GI (SOGI) based structure is easy to implement due to its structural simplicity. However, it suffers from poor harmonics and DC-offset rejection capabilities. Two improved structures are reported for DC-offset mitigation, one consisting of a dedicated loop to reject the DC-offset, while the other uses two cascaded SOGIs. The improved structure is effective in rejecting the DC-offset, but they are still inefficient in mitigating dominant lower order harmonics. Although the harmonic rejection capability can be improved by reducing the filter's bandwidth, it affects the dynamic response, and there is always a compromise between steady-state and dynamic performance of the system. To overcome this, this work proposes a hybrid multi-resonant GI structure consisting of multiple layers. The first layer consists of cascaded SOGI, which rejects the DC-offset, while the other layers facilitate selective harmonic elimination (SHE) by tuning filters to the particular harmonic component. Thus, the proposed control structure can mitigate both DC-offset and dominant lower harmonic, as demonstrated using frequency domain analysis through Bode plot. A frequency-locked loop (FLL) is incorporated to make the system tolerant to any frequency variation. The effectiveness of the proposed control structure is authenticated via simulation studies under different grid abnormalities. Electric drive used in the SWP system to run. This technique eliminates the need for speed sensors, making the system more robust and reliable. Various types of electric drives have been utilized for SWP, starting from brushed DC motor to the latest permanent magnet synchronous motor (PMSM). Induction motors have been used for SWP for a long time but are not suitable for smaller rating machines due to their reactive power demand and low efficiency. Recent advancements in high-density permanent magnet materials have led to the development of PMSM, which has permanent magnets on their rotor and is free from rotor copper losses. PMSM offers high efficiency, high torque to weight ratio, fast dynamic response, and smaller size, making it the best-suited electric drive for SWP. The presented work implements a sensor-less vector control technique for controlling the speed of the PMSM, which improves system reliability and reduces system cost. The hybrid multi-resonant generalized integrator-frequency locked loop (HMRGI-FLL) control structure is used to filter abnormal grid voltage and extract its fundamental component. PQ issues, such as voltage sag, voltage swell, grid current distortion, and grid voltage distortion, are mitigated to ensure that the presented system follows the IEEE standard for PQ in grid-connected systems.

III. SYSTEM ARCHITECTURE

The arrangement of the grid integrated SWP system employing PMSM drive is presented in Figure 1. The said system is comprised of a solar photovoltaic (PV) array, a boost converter that facilitates maximum power point tracking (MPPT), a voltage source inverter (VSI) that propels the motor, an additional boost front end converter (FEC), and a PMSM that is connected to a pump. The velocity of the PMSM is controlled through a sensor-less vector control method. MPPT is achieved by utilizing an incremental conductance (INC) algorithm that alters the duty ratio of switch Sb. The grid supplies DC link by means of the FEC converter. The correct operation of switch SFEC permits the transfer of power from the grid. To eliminate switching harmonics and current ripples, an RC filter (Rf, Cf) and an interfacing inductor (Lf) are employed, respectively. The functioning of the WPS is verified by experimental analysis of the system constructed in the laboratory, in various operating conditions

III. SYSTEM OPERATION AND CONTROL

The operation of the proposed SWP system is divided into two modes. First mode is the grid connected mode, which is enabled when utility grid is available. Whereas, the second mode is the standalone mode, which is enabled when the grid is not available. When the SWP system is connected to the grid, the speed of the pump is regulated at the nominal speed and the excess power in addition that generated from solar PV array is supplied from the grid. In order to make the WPS operable even under weak grid scenarios, a HMRGI-FLL based structure is utilized. The HMRGI-FLL structure extracts the fundamental component from the polluted grid voltage, which is utilized for the generation of unit



template. The unit template is multiplied with weight component for the generation of sinusoidal reference grid current. The switching of FEC is controlled in accordance with reference grid current such that the grid current remains sinusoidal. When grid is unavailable, the pump speed changes in accordance to the change in solar insolation. The control of the WPS is divided into three parts. First is MPPT control using INC MPPT algorithm. Second is the speed control of PMSM using sensor-less vector control technique as shown in Fig. 2. A stationary stator flux observer based method is adopted here for speed and position estimation. The third is power flow control from the utility grid. This is achieved using HMRGI-FLL based control technique.

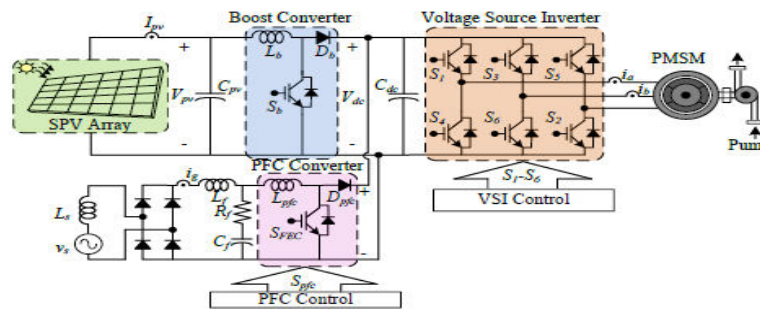


Fig. 1 System Configuration

A. MPPT

An INC algorithm is one of the commonly used technique for MPPT. The MPPT algorithm controls the duty ratio such that the instantaneous conductance is equal to the incremental conductance. It provides a fast MPP tracking even under rapidly changing environmental conditions.

B. Estimation of Rotor Speed and Position

The information of PMSM position and speed are needed for the regulation of PMSM speed. An encoder can easily furnish these informations, however, due to complexity and cost involved, their use is not recommended for submersible water pumping. The harsh surrounding conditions faced by the submersible pumps lead to serious reliability issues owing to the introduction of encoder. The use of lengthy cable for transmitting high frequency low amplitude encoder signals from encoder to the controller, pollutes them and restrict them to surface water pumping. Therefore, a stationary flux observer based rotor position and speed estimation using SOGI-FLL, presented in for sensorless operation of an induction motor is adopted here for speedcontrol of Permanent Magnet Synchronous Motor(PMSM).

The back emf in stationary reference frame (e_{sa} , $e_{s\beta}$) for a PMSM, is given as,

$$e_{sa} = v_a - R_s * i_a, e_{s\beta} = v_\beta - R_s * i_\beta \quad (1)$$

where, (v_a , v_β) and (i_a , i_β) are the stationary reference frame voltages and currents, R_s is the stator winding resistance. The stationery components of stator flux (ψ_α , ψ_β) are estimated using SOGI-FLL structure. The output of the SOGIFLL structure is expressed as

$$\varphi_{\alpha\beta} = \frac{k\omega_{mest}}{s^2+k\omega_{mest}s+\omega_{mest}^2} * e_{s\alpha\beta} \quad (2)$$

where, ω_{mest} is the estimated electrical frequency in rad/sec. The resultant flux linkage (ψ_s) is calculated as,

$$\varphi_s = \sqrt{\varphi_\alpha^2 + \varphi_\beta^2} \quad (3)$$

The estimated electrical position (θ_{est}) is expressed as,

$$\theta_{est} = \tan^{-1} \frac{\varphi_\beta}{\varphi_\alpha} \quad (4)$$

The estimated rotor speed (ω_{mest}) is calculated as,

$$\omega_{mest} = \frac{1}{p} \frac{d}{dt} (\theta_{est}) = \frac{\varphi_\alpha \cdot \dot{\varphi}_\beta - \varphi_\beta \cdot \dot{\varphi}_\alpha}{p \varphi_s^2} \quad (5)$$

where, p is the number of pole pairs, $\dot{\varphi}_\alpha$ is the derivative of φ_α and $\dot{\varphi}_\beta$ is the derivative of φ_β . Owing to the grid



integration of the WPS, scenarios can be visualized the grid is available and grid failure. When the grid is available (i.e. $V_t \geq V_{th}$), the pump is set to operate at its nominal values and the DC link voltage is regulated by the boost FEC.

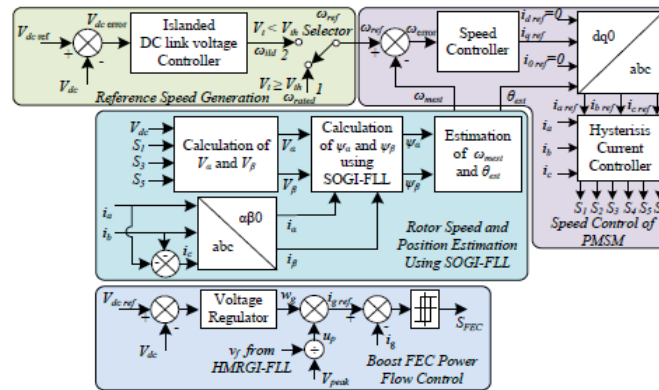


Fig. 2 Control scheme for the proposed SWP system

However, during grid failure (i.e. $V_t < V_{th}$), the DC link voltage (V_{dc}) is controlled using islanded V_{dc} controller and is expressed as

$$\omega_{ref} = \left(K_{pidc} + \frac{K_{iadc}}{s} \right) \{ V_{dcref}(k) - V_{dc}(k) \} \quad (6)$$

where, K_{pidc} and K_{iadc} are proportional and integral gains of islanded V_{dc} controller. The V_{th} is selected as 70% of the nominal V_t .

The speed of the PMSM is regulated through the speed controller. The error generated by comparing ω_{ref} and ω_{mest} is fed to the speed controller. Its output is considered as reference quadrature axis current (i_q ref) expressed as,

$$i_{qref}(k) = \left(K_{p\omega} + \frac{K_{i\omega}}{s} \right) \{ \omega_{ref}(k) - \omega_{mest}(k) \} \quad (7)$$

where, $K_{p\omega}$ and $K_{i\omega}$ are the controller gains. For SWP operation, the pump speed is limited to its rated value. Therefore, the reference current of the direct axis (i_d ref) is set at zero.

The reference currents of the PMSM i_a ref, i_b ref and i_c ref are attained from i_d ref and i_q ref through the inverse Park's transform. The gating pulses (S_1 - S_6) are generated by comparing the reference and sensed motor currents (i_a , i_b and i_c) using hysteresis controller.

C. Grid Power Flow Control

The control of grid power flow is visualized through the control technique depicted in Fig. 2. During grid availability, the voltage regulator controls V_{dc} by feeding the error of reference and sensed V_{dc} into it. The voltage regulator output is the weight component (w_g) and is expressed as.

$$w_g(k) = \left(K_{pdc} + \frac{K_{idc}}{s} \right) \{ V_{dcref}(k) - V_{dc}(k) \} \quad (8)$$

where, K_{pdc} and K_{idc} are proportional and integral gains of the voltage regulator.

The HMRGI-FLL control structure shown in Fig. 3, is utilized for grid voltage filtering. It rejects the harmonics and DC-offset in the grid voltage and generates a fundamental frequency unit template (u_p) even under abnormal grid conditions. The u_p expressed as,

$$u_p = |v_f| / V_{peak} \text{ where, } v_f \text{ is the magnitude of fundamental grid voltage (} v_f \text{) and } V_{peak} \text{ is the peak grid voltage (} V_{peak} \text{) expressed as,}$$

$$V_{peak} = \sqrt{v_f^2 + qv_f^2}$$

The reference grid current (i_{gref}) is the product of w_g and unit template (u_p) and is expressed as,

$$i_{gref} = w_g * u_p(i_g)$$

The error between i_{gref} and sensed grid current (i_g) are utilized for generating the FEC switching signal as depicted in Fig. 2.



IV. ANALYSIS OF HMRGI-FLL

For proper operation even during abnormal grid conditions, first the grid voltage is filtered using the proposed HMRGI-FLL structure shown in Fig. 3. The HMRGI-FLL control structure consists of multiple layers. The first layer consists of cascaded SOGI (CSOGI), which rejects the DC-offset and provides band pass filtering, whereas, the other layers facilitate SHE using SOGI structure through tuning of filters to the particular harmonic component. Since in a 1-φ system the 3rd, 5th and 7th harmonic components are found to be dominant, therefore, they are filtered through SHE filters and are eliminated using harmonic decoupling network. Thus the proposed control structure provides an enhanced filtering and is capable of mitigating both, DC-offset as well as dominant lower harmonic. The transfer function (TF) for SOGI is given as

$$D_{SOGI} = \frac{v_f(s)}{v(s)} = \frac{k\omega's}{s^2 + k\omega's + \omega'^2}$$

$$Q_{SOGI} = \frac{qv_f(s)}{v(s)} = \frac{k\omega's}{s^2 + k\omega's + \omega'^2}$$

where, ω' is the grid frequency and k = 2ζ, ζ is the damping factor. The value of ζ regulates the settling time ts. The ts is expressed as,

$$t_s = 4/(\zeta\omega')$$

The value of ζ lies within 0 and 1. The TF for CSOGI is written as

$$D_{CSOGI} = \frac{v_f(s)}{v(s)} = \frac{c_1c_2\omega'^2s^2}{(s^2 + c_2\omega's + \omega'^2)(s^2 + \omega'^2) + c_1c_2\omega'^2s^2}$$

$$Q_{CSOGI} = \frac{qv_f(s)}{v_s(s)} = \frac{c_1c_2\omega'^3s}{(s^2 + c_2\omega's + \omega'^2)(s^2 + \omega'^2) + c_1c_2\omega'^2s^2}$$

The TFs for in-phase and quadrature-components of HMRGI-FLL, are given..

The performance analysis of HMRGI-FLL is presented in Fig. 4 show frequency domain analysis, where it can be realized that HMRGI-FLL effectively filters the fundamental frequency component and rejects the components of all other frequency. It can be perceived from the frequency plot for in-phase and quadrature components that along with DC-offset rejection, the presented structure can effectively eliminated dominant 3rd, 5th and 7th harmonic component through SHE.

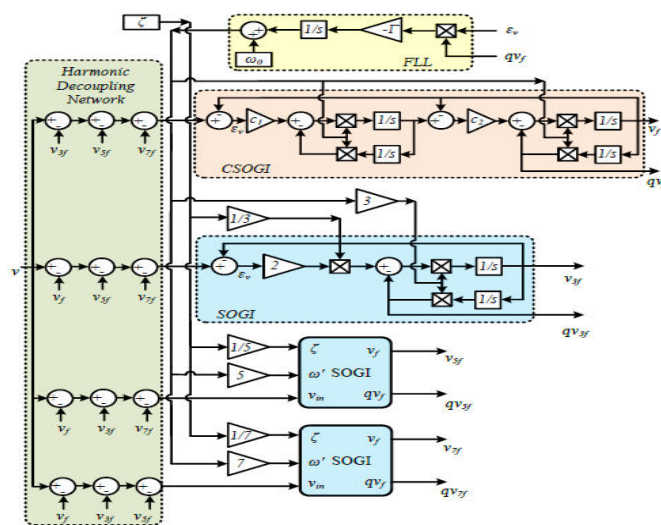


Fig.3 Structure of HMRGI-FLL



$$D_{HMRGI-FLL} = \frac{v_f(s)}{v(s)} = \left[\begin{array}{c} D_{CSOGI} \left(\frac{1 - D_{SOGI3}(s)}{1 - D_{SOGI3}(s)D_{CSOGI}(s)} \right) \\ \left(\frac{1 - D_{SOGI5}(s)}{1 - D_{SOGI5}(s)D_{CSOGI}(s)} \right) \left(\frac{1 - D_{SOGI7}(s)}{1 - D_{SOGI7}(s)D_{CSOGI}(s)} \right) \end{array} \right]$$

$$Q_{HMRGI-FLL} = \frac{qv_f(s)}{v(s)} = \left[\begin{array}{c} Q_{CSOGI} \left(\frac{1 - Q_{SOGI3}(s)}{1 - Q_{SOGI3}(s)Q_{CSOGI}(s)} \right) \\ \left(\frac{1 - Q_{SOGI5}(s)}{1 - Q_{SOGI5}(s)Q_{CSOGI}(s)} \right) \left(\frac{1 - Q_{SOGI7}(s)}{1 - Q_{SOGI7}(s)Q_{CSOGI}(s)} \right) \end{array} \right]$$

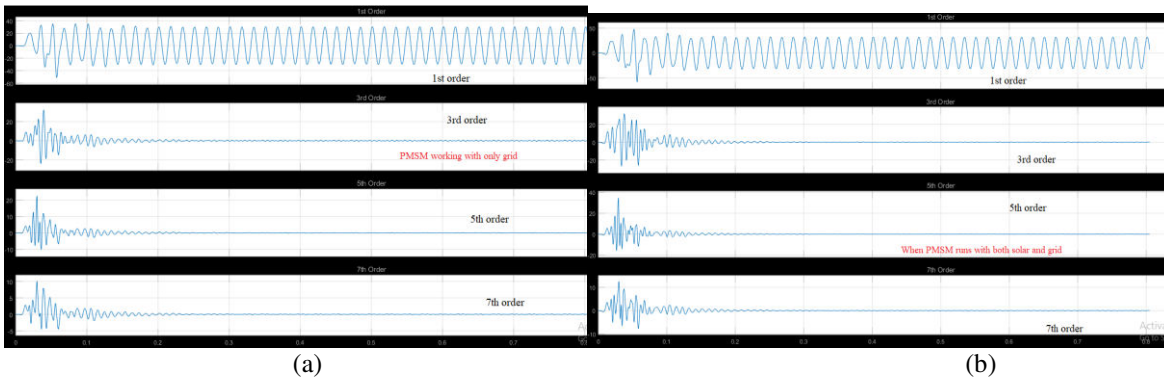


Fig 4. Performance of HMRGI-FLL
 (a) Harmonics during PMSM working with grid
 (b) Harmonics during PMSM working with both grid and solar at 500w/m²

V. POWER QUALITY PERFORMANCE OF GRID

The power quality performance of SWP system, is depicted in Fig.5(a) .The Power Quality performance when the grid alone is feeding the pump. During this condition, the grid feeds a power to run the pump at rated speed. The Power Quality performance when the grid and PV array, both are feeding the pump and solar insolation is kept at 500 W/m² is shown in Figs.5(b) The grid feeds a partial power of 1.26 kW during this scenario. The grid current total harmonic distortion (THD) is found to be 2.7% and 4.5% under both the above conditions, which is well within the specified limit of 5% stated. We observed that THD_Current of 3.83% which is in the limited range.

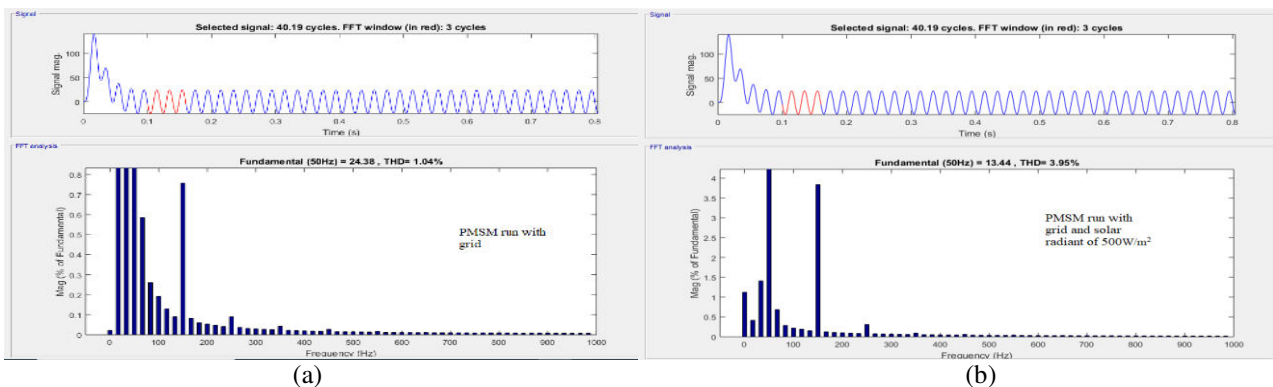


Fig 5. Waveforms Of THD-CURRENT
 (a) PMSM working only with grid
 (b) PMSM working with both grid and solar



VI. WORKING OF MODEL

In this model we use two power sources one is renewable energy source i.e.,Solar energy and second source is Grid.The operation of the proposed SWP system is divided into three modes

- 1: PMSM works only with solar
- 2: PMSM works only with grid
- 3: PMSM works with both grid and solar

Case 1: when PMSM working with solar:

In condition the solar radiant is fixed to 1000w/m² to and grid volatge to zero to run PMSM only though solar.The boost converter increase the outputvoltage of solar panel to maximum volatge required to run the PMSM.The output voltage of booster conerteris DC link voltage(Vdc).The voltage of solar panel is Vpv and current is Ipv.The grid current is Ig and voltage is Vg.The dc supply converted into ac to run the PMSM.The Fig .6 shows the output of simulink model.By this we conclude that the motor can also run at rated speed with the solar input

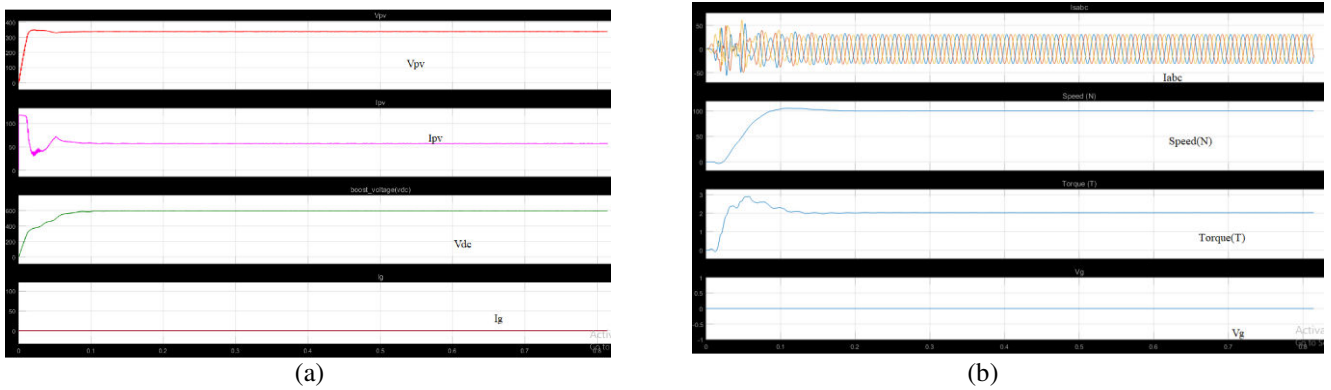


Fig 6.Output of Simulink Model During Solar input

.Case 2: When PMSM works only with grid

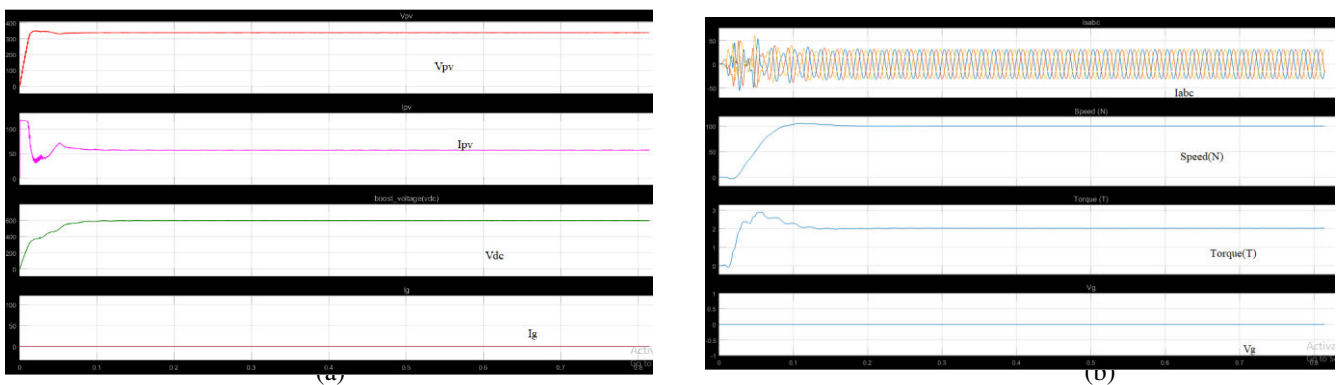


Fig 7.Output of Simulink model During Grid input

In this condition the solar radiant is set to 0 W/m² and the grid is set to maximum voltage of 230V.The rectifier is used to convert ac into dc.Booster converter gives a minimum input in the absence of the solar.The HMRGI-FLL used to reduce the odd harmonics present in the supply.The PMSM is worked on ac supply only.So we use a inverterto convert dc into ac.The Fig.7 shows the output of Simulink model with grid supply.By this the PMSM can run at rated speed in absence of solar.

Case-3: When PMSM works with both solar and grid

In this condition the solar radiant is set to 500 W/m^2 and the grid help to run the PMSM. The boost converter increase the solar voltage, the voltage output of boost converter is called DC link voltage (V_{dc}). The voltage from the grid is converted into DC with the help of 1-phase bridge rectifier. The HMRGI-FLL is used to reduce the distortion of odd harmonics. The DC voltage converted into AC and supplied to PMSM. The Fig.8 shows the output of the Simulink model with both solar and grid supplies. By this we observe that if the solar generate less power than the requirement the grid supplies the excessive power and run the motor.

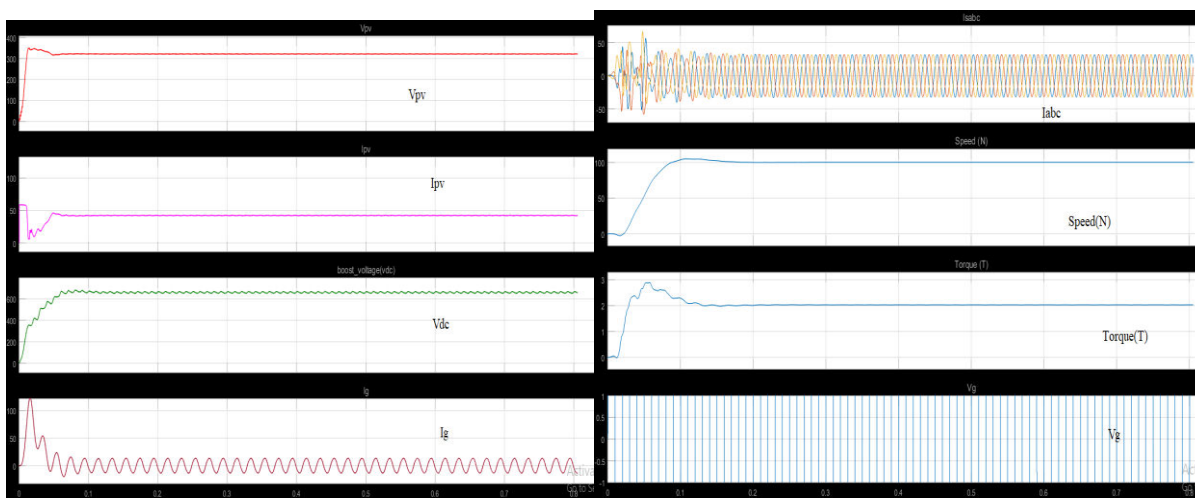


Fig 8. Output of Simulink Model with both solar and grid

VII. CONCLUSION

We observed that our proposed model can work in solar or grid or both supplies. Of this, the use of renewable energy increases, and the grid is used for backup and works when the absence of solar. The performance of HMRGI-FLL is validated through simulation studies under various grid abnormalities and is satisfactory. The frequency domain analysis has revealed the effectiveness of the HMRGI-FLL structure. The boost FEC converter has expedited the power flow from the grid while enhancing the PQ performance at the grid terminals. The use of HMRGI-FLL has removed the distortion in the grid current and kept the current THD within the specified limits, even if the grid voltage is distorted. The elimination of the speed sensor reduces the overall system cost. Therefore, this WPS offers a feasible solution for reliable solar water pumping. By this model can reduce the cost of electricity bill and also we can use store the energy or fed power to grid to generate income from solar energy.

REFERENCES

1. S. Murshid and B. Singh, "Implementation of PMSM drive for a solar water pumping system," IEEE Trans. Ind. Appl., vol. 55, no. 5, pp. 4956- 4964, Sept.-Oct. 2019.
2. Jain, R. Karampuri and V. T. Somasekhar, "An integrated control algorithm for a single-stage PV pumping system using an open-end winding induction motor," IEEE Trans. Ind. Elect., vol. 63, no. 2, pp. 956- 965, 2016.
3. Khiareddine, C. Ben Salah and M. F. Mimouni, "Strategy of energy control in PVP/battery water pumping system," in Proc. International Conf. on Green Energy, Sfax, 2014, pp. 49-54.
4. P. García, C. A. García, L. M. Fernández, F. Llorens and F. Jurado, "ANFIS-based control of a grid-connected hybrid system integrating renewable energies, hydrogen and batteries," IEEE Trans. Ind. Info., vol. 10, no. 2, pp. 1107-1117, May 2014.
5. Ducar and C. Marinescu, "Increasing the efficiency of motor-pump systems using a vector controlled drive for PMSM application," in proc. Int. Symp. on Fund. of Electrical Engg. (ISFEE), Bucharest, 2014, pp. 1- 5.
6. B. C. S. B. Slama and A. Chrif, "Efficient design of a hybrid (pv-fc) water pumping system with separate mppt control algorithm," IJCSNS Int. J. of Comp. Science and Net. Security, vol.12, pp. 53-60, January 2012.



7. S. Murshid and B. Singh, "Utility grid interfaced solar water pumping system using PMSM drive," in proc. IEEE Int. Conf. on Pow. Elect., Drives and Energy Syst. (PEDES), Chennai, India, pp. 1-6, 2018.
8. R. Kumar and B. Singh, "Grid interactive solar PV-based water pumping using BLDC motor drive," IEEE Trans. Ind. Appl., vol. 55, no. 5, pp. 5153-5165, Sept.-Oct. 2019.
9. B. Singh and S. Murshid, "A grid-interactive permanent magnet synchronous motor driven solar water-pumping system," IEEE Trans. Ind. Appl., vol. 54, no. 5, pp. 5549-5561, Sept.-Oct. 2018.



INNO SPACE
SJIF Scientific Journal Impact Factor
Impact Factor
7.54

ISSN

INTERNATIONAL
STANDARD
SERIAL
NUMBER
INDIA



INTERNATIONAL JOURNAL OF MULTIDISCIPLINARY RESEARCH IN SCIENCE, ENGINEERING AND TECHNOLOGY

| Mobile No: +91-6381907438 | Whatsapp: +91-6381907438 | ijmrset@gmail.com |

www.ijmrset.com